

A Full Compensating System for General Loads, Based on a Combination of Thyristor Binary Compensator, and a PWM-IGBT Active Power Filter

Juan Dixon, *Senior Member, IEEE*, Yamille del Valle, Marcos Orchard, Micah Ortúzar, Luis Morán, *Senior Member, IEEE*, and Carlos Maffrand

Abstract—A full compensating system for distribution networks, able to eliminate harmonics, correct unbalanced loads, and generate or absorb reactive power, is presented. The system is based on a combination of a thyristor binary compensator (TBC), and a pulsewidth-modulation insulated gate bipolar transistor active power filter (APF) connected in cascade. The TBC compensates the fundamental reactive power and balances the load connected to the system. The APF eliminates the harmonics and compensates the small amounts of load unbalances or power factor that the TBC cannot eliminate due to its binary condition. The TBC is based on a chain of binary-scaled capacitors and one inductor per phase. This topology allows, with an adequate number of capacitors, a soft variation of reactive power compensation and a negligible generation of harmonics. The capacitors are switched on when the line voltage reaches its peak value, avoiding inrush currents generation. The inductor helps to balance the load, and absorbs reactive power when required. The APF works measuring the source currents, forcing them to be sinusoidal. The two converters (TBC and APF) work independently, making the control of the system simpler and more reliable. Simulations show that the system is able to respond to many kinds of transient perturbations in no more than a couple of cycles. The paper analyzes the circuit proposed, the way it works and shows some experimental results obtained under operation.

Index Terms—Power conditioners, power electronics, power filters, reactive power control.

I. INTRODUCTION

LOAD compensation, in distribution networks, is oriented to solve three different problems: reactive power compensation, unbalanced loads correction, and harmonic elimination.

For reactive power compensation, different strategies and topologies have been used: synchronous machines, capacitor banks, static var compensators (SVCs) [1], and pulsewidth-modulation (PWM) compensators [2], [3]. However, most of them have disadvantages: synchronous machines

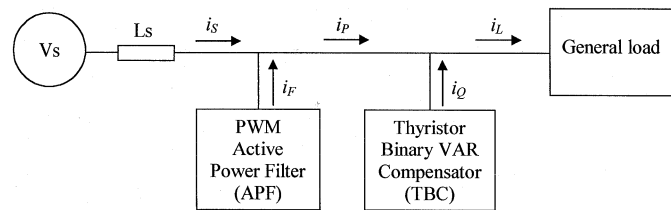


Fig. 1. Proposed topology.

are bulky and have a poor dynamic behavior, and capacitor banks have inrush problems during connection and disconnection [4], SVCs are harmonic polluters and PWM compensators are still expensive and complicated for high power levels. On the other hand, unbalance problems cannot be solved using synchronous machines, but a solution can be obtained with a combination of reactors and capacitors [1], or with PWM compensators. For harmonic elimination, the solution comes from the use of PWM shunt active power filters [5], [6], but at a high cost for high-power applications. To lower the cost of using PWM techniques, series active power filters [6] and combined topologies such as shunt passive filters with series active filters, shunt passive with active filters or converters connected in cascade have been proposed [7], [8]. However, cost is still a problem when insulated gate bipolar transistors (IGBTs) or gate turn-off thyristors (GTOs) are used for high-power applications.

This paper presents a simple topology, which is shown in Fig. 1. This topology can be used in high power for full compensation of the aforementioned problems. The system consists of a combination of thyristor binary compensator (TBC) [10], [11] operating in cascade with an active power filter (APF) [12]. In this configuration the TBC solves the power factor and unbalance problems for high power levels, by producing pure sinusoidal currents while the APF, working in medium power level, gives the solution for harmonics cancellation problem.

The proposed topology has the following distinctive characteristics: 1) it compensates power factor, unbalanced loads, and harmonics; 2) it can compensate three phase loads in a minimum of two cycles; 3) the APF and TBC work independently, and an individual control strategy is used for each equipment; and 4) inrush problems during connection and/or disconnection of capacitors are avoided by keeping the appropriate conditions of

Manuscript received <AUTHOR: DATES CORRECT?> February 6, 2002; revised January 15, 2003. This work was supported by Conicyt under Fondecyt Project 1020460.

J. Dixon, Y. del Valle, M. Orchard, and M. Ortúzar are with the Department of Electrical Engineering, Pontificia Universidad Católica de Chile, Santiago, Chile (e-mail: jdixon@ing.puc.cl).

L. Morán is with the University of Concepción, Concepción, Chile.

C. Maffrand is with the University of Río Cuarto, Río Cuarto, Argentina.

Digital Object Identifier 10.1109/TIE.2003.817604

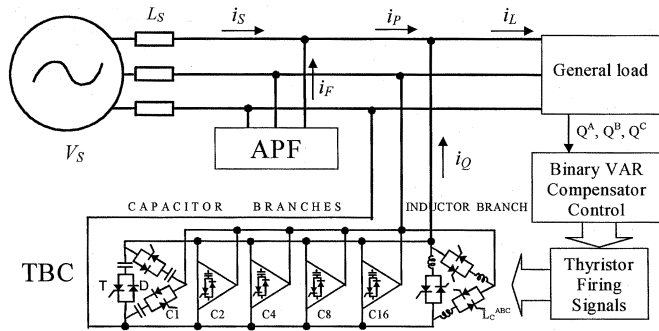


Fig. 2. Configuration for TBC equipment.

“null initial current” and “null voltage” between connection terminals.

II. PROPOSED TOPOLOGY DESCRIPTION

The proposed topology for the interconnection between TBC and APF is shown in Fig. 1. This configuration ensures that TBC and APF can work independently, in the satisfaction of well-delimited objectives.

The TBC equipment measures the fundamental components of the load line currents “ i_L ,” and calculates the value for the susceptances, necessary to connect between each phase of the electrical system, to get unity-power-factor operation, and a balanced load referred to the main voltage source.

On the other hand, the APF [12] measures the line source currents “ i_s ” and injects the harmonic components “ i_F ” necessary to obtain a sinusoidal waveform in the main source current. Additionally, “ i_F ” contains the small amounts of reactive power that the TBC cannot eliminate due to its binary operation.

The operation principle for each equipment is analyzed in the following sections.

A. TBC

The topology of the TBC is shown in Fig. 2, and consists of variable susceptances, connected in delta configuration, through common cathode, antiparallel, thyristor-diode connection. The variability of each susceptance is based on a chain of binary-scaled capacitors and one inductor, whose value is chosen according to the reactive power that the capacitors can generate if they are all connected.

The presented topology allows for the injection or absorption of the amounts of reactive power $B^{(c)}_{ab}$, $B^{(c)}_{bc}$ and $B^{(c)}_{ca}$ that are required in a three-phase electrical system to obtain unity power factor operation, and a balanced load in the main source terminals. Additionally, the configuration allows having a dynamic compensation range of $[-Q, Q]$ in each phase where Q is the maximum reactive power that the capacitors can generate.

Since the values of capacitors are selected as binary scaled, it is possible to obtain a linear regulation of compensating reactive power, by connecting or disconnecting them in the appropriate sequence. The precision of regulation is established by the lowest capacitor value [10].

The appropriate conditions for the connection of capacitors or inductances must keep the requirements of “null initial current”

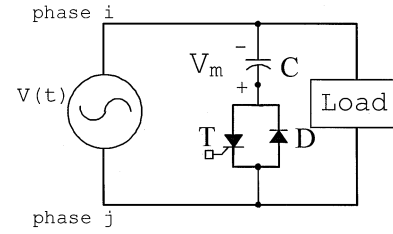


Fig. 3. Capacitor connection topology.

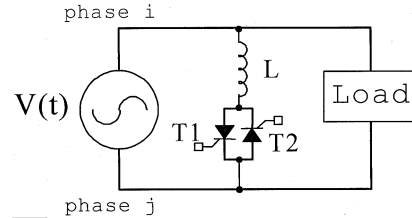


Fig. 4. Inductor connection topology.

and “null voltage between connection terminals” to prevent in-rush currents.

Considering the topology shown in Fig. 3 for each capacitor, when the thyristor T is “off” the diode D keeps the capacitor C charged at the peak negative value of the main supply ($-V_m$) which in this case corresponds to the negative peak of phase-to-phase voltage. The optimal firing moment for the capacitor is given by the following equations:

$$v^{Th}(t) = v(t) - V_c = V_m \sin(\omega t) - V_c \quad (1)$$

where

- v^{Th} thyristor voltage;
- $v(t)$ main source phase-to-phase voltage;
- V_c capacitor’s voltage;
- V_m peak value of $v(t)$.

In the connection moment,

$$v^{Th}(t) = v(t) - V_c = V_m (\sin(\omega t) + 1) = 0. \quad (2)$$

According to (2), a soft connection is obtained when the main supply reaches its maximum negative voltage ($\omega t = 270^\circ$). Then, the capacitor current will increase from zero following (3)

$$i_c = C \cdot V_m \cdot \frac{d}{dt} (-\cos(\omega t)) = C \cdot V_m \sin(\omega t). \quad (3)$$

A similar analysis could be made for the current in the inductance connected between each phase. In this case, the configuration is given by Fig. 4, where two thyristors are required instead of one. In this case, it is required to fire each thyristor, $T1$ and $T2$, in the negative and positive peak of the supply voltage (phase-to-phase voltage), respectively.

The value of the susceptances that must be connected, to obtain the power-factor correction and load balance, can be calculated by an analysis of the zero, positive, and negative sequences of the current set. The compensation objective can be stated as

to eliminate the negative-sequence component (balancing) and to cancel the reactive component of positive sequence, considering a null zero-sequence phasor [1].

The expressions for the reactive requirements $B^{(c)}_{ab}$, $B^{(c)}_{bc}$ and $B^{(c)}_{ca}$, that are obtained from the aforementioned method, are given by (4)–(6)

$$B^{(c)}_{ab} = k \cdot \left(-\frac{1}{\sqrt{3}} \cdot \text{Im}(I_{a1}) - \frac{1}{\sqrt{3}} \cdot \text{Im}(I_{a2}) + \text{Re}(I_{a2}) \right) \quad (4)$$

$$B^{(c)}_{bc} = k \cdot \left(-\frac{1}{\sqrt{3}} \cdot \text{Im}(I_{a1}) + \frac{2}{\sqrt{3}} \cdot \text{Im}(I_{a2}) \right) \quad (5)$$

$$B^{(c)}_{ca} = k \cdot \left(-\frac{1}{\sqrt{3}} \cdot \text{Im}(I_{a1}) - \frac{1}{\sqrt{3}} \cdot \text{Im}(I_{a2}) - \text{Re}(I_{a2}) \right) \quad (6)$$

where

$$k = \frac{1}{\sqrt{3} \cdot V}.$$

Equations (4)–(6) can be expressed as the following time variation [1]:

$$B^{(c)}_{ab} = -\frac{1}{\sqrt{3} \cdot V_{ff \text{ peak}}} \times \left[i_a(t) \left. \frac{dV_a}{dt} > 0 \right|_{V_a(t)=0} + i_b(t) \left. \frac{dV_b}{dt} > 0 \right|_{V_b(t)=0} - i_c(t) \left. \frac{dV_c}{dt} > 0 \right|_{V_c(t)=0} \right] \quad (7)$$

$$B^{(c)}_{bc} = -\frac{1}{\sqrt{3} \cdot V_{ff \text{ peak}}} \times \left[i_b(t) \left. \frac{dV_b}{dt} > 0 \right|_{V_b(t)=0} + i_c(t) \left. \frac{dV_c}{dt} > 0 \right|_{V_c(t)=0} - i_a(t) \left. \frac{dV_a}{dt} > 0 \right|_{V_a(t)=0} \right] \quad (8)$$

$$B^{(c)}_{ca} = -\frac{1}{\sqrt{3} \cdot V_{ff \text{ peak}}} \times \left[i_c(t) \left. \frac{dV_c}{dt} > 0 \right|_{V_c(t)=0} + i_a(t) \left. \frac{dV_a}{dt} > 0 \right|_{V_a(t)=0} - i_b(t) \left. \frac{dV_b}{dt} > 0 \right|_{V_b(t)=0} \right] \quad (9)$$

where $i_a(t) \left. \frac{dV_a}{dt} > 0 \right|_{V_a(t)=0}$ represents the measure of current i_a in the instant where the line voltage V_a has its zero-crossing point (positive slope).

The calculated values for the susceptances must consider

$$B^{(c)}_{ij} = \omega C_{ij}, \quad \text{if } B^{(c)}_{ij} \geq 0 \quad (10)$$

$$B^{(c)}_{ij} = (\omega L_{ij})^{-1}, \quad \text{if } B^{(c)}_{ij} < 0 \quad (11)$$

where C_{ij} is the capacitor connected in the branch between phase “ i ” and “ j ,” and L_{ij} is an equivalent inductance connected between phases “ i ” and “ j .”

The equations stated in (7)–(11) make possible the implementation of a real-time control methodology based on the measurements of line load currents.

The previously mentioned concepts are still valid if the TBC equipment is configured in star connection. In this case, it is necessary to consider the following expression to transform the delta susceptances in the star susceptances that must be connected between each phase and ground:

$$B_{in}^{-1} = \frac{B_{ij}^{-1} \cdot B_{ki}^{-1}}{B_{ij}^{-1} + B_{jk}^{-1} + B_{ki}^{-1}} \quad (12)$$

where

B_{in}^{-1} susceptance between phase “ i ” and ground;

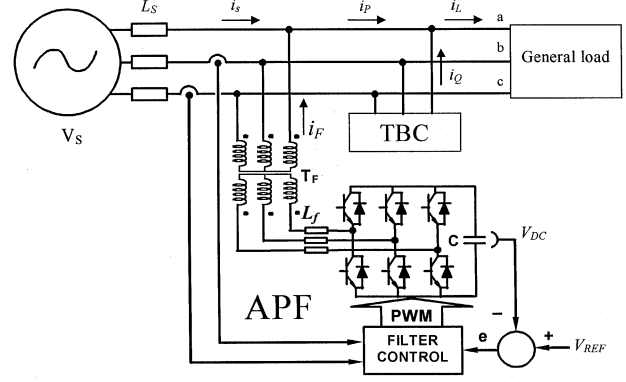


Fig. 5. Configuration for APF equipment.

B_{ij}^{-1} susceptance between phases “ i ” and “ j ”;
 B_{jk}^{-1} susceptance between phases “ j ” and “ k ”;
 B_{ki}^{-1} susceptance between phases “ k ” and “ i ”.

B. APF

The shunt configuration for an APF, as shown in Fig. 5, is considered in the proposed topology. It is used as a current source, to maintain sinusoidal current waveforms in the main voltage supply. The APF uses the current-hysteresis-controller method, and works as follows: the error signal “ e ” coming from $(V_{REF} - V_{DC})$, generates from a proportional–integral (PI) controller, a current magnitude signal I_{MAX} . This signal is multiplied by a sinusoidal reference in phase with the mains voltage supply V_S producing a sinusoidal current reference template. In this way, as the current sensors of the APF are connected at the supply side, these currents are forced to follow this sinusoidal template whose amplitude allows keeping the filter voltage V_{DC} at the reference voltage V_{REF} . This operation is independent of waveform and magnitude of the current i_P (see Fig. 1).

Therefore, the APF equipment is able to generate the current “ i_F ,” which contains three basic components [see (13)]. The first component “ i_{Fd} ” is in phase with the main voltage supply, and only exists a small amount for power loss compensation into the APF. The second component “ i_{Fq} ” is in quadrature with V_S and compensates residual Q that has not been taken by the TBC. The last, “ i_{Fh} ,” has the harmonic components and is the most important component for the APF [12]

$$i_F = i_{Fd} + i_{Fq} + \sum_h i_{Fh} \quad (13)$$

$$i_F = I_{Fd} \sqrt{2} \sin(\omega t) + I_{Fq} \sqrt{2} \cos(\omega t) + \sum_h I_{Fh} \sqrt{2} \sin(h\omega t - \phi_h).$$

The APF, working in a medium power level, is connected to the high-voltage network through a three-phase transformer. This configuration allows reducing the cost associated to APF design, and avoids the utilization of force-commutated semiconductors at high voltage levels. The ratio between rated power of IGBT’s and thyristors depends on the size of the compensating capacitors located in the “C1” branch of the TBC. They define the reactive power step that has to be compensated by the APF. Besides it also depends on the magnitude of harmonics

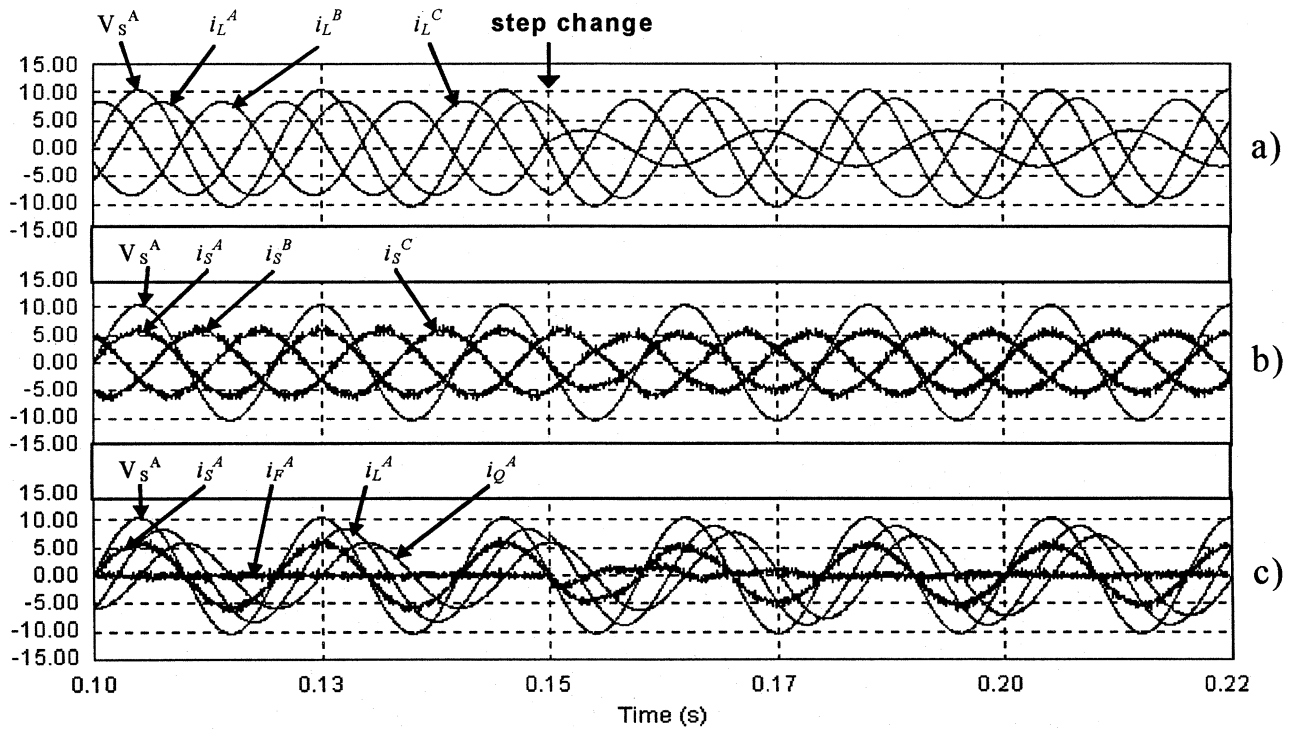


Fig. 6. Step response from lagging balance load to unbalanced load. (a) Load currents. (b) Source currents. (c) Phase “a” currents.

generated by the load because the TBC only compensates fundamental reactive power.

The inductance “ L_f ” is a current slope limiter of the currents injected to the network and it is essential in the protection of the semiconductor components (IGBTs), and in the absorption of the instantaneous voltage differences between the system and the output of the APF.

The control strategy applied to the APF is based on the analysis of its electrical behavior. In fact, it is possible to obtain an expression that represents the power balance under the required conditions for line supply currents. That is, when the *rms* values of the currents “ i_s ” are balanced, and have unity power factor and no harmonic components

$$p_s = P_s = P_{\text{load}} - P_f = 3V \cdot i_s^{\text{rms}} = P_{\text{load}} - \frac{\Delta W_c}{T} \quad (14)$$

$$\hat{p}_f = \hat{p}_{\text{load}} \quad (15)$$

where

- p_s instantaneous power at source terminals;
- P_s average active power at source terminals;
- P_{load} average active power at load;
- P_f average active power at APF equipment;
- $(\Delta W_c/T)$ average power in APF capacitor;
- \hat{p}_f instantaneous var and harmonic power in APF;
- \hat{p}_{load} instantaneous var and harmonic power at load.

Therefore, the control of the APF must satisfy (14) and (15) to obtain the required operating conditions. Even more, from (14) it is possible to find an expression for the supply currents

“ i_s^{rms} ,” in terms of the average power variation in the APF capacitor

$$i_s^{\text{rms}} = \frac{1}{3V} \left[P_{\text{load}} - \frac{\Delta W_c}{T} \right] = \frac{1}{3V} \left[P_{\text{load}} - \frac{C}{2T} \Delta V_{DC}^2 \right]. \quad (16)$$

Then, the control method can be based on a PI closed loop, which forces the line supply currents “ i_s ” to be sinusoidal and in phase with the corresponding main voltages. The PI controller keeps the APF capacitor voltage “ V_{DC} ” according to a reference “ V_{REF} ,” by manipulating the amplitude of “ i_s .”

If the real value of “ i_s^{rms} ” is different from $P_{\text{load}}/(3V)$, the capacitor voltage will increase or decrease according to expression (16). The controller calculates the value the line supply currents must have, to keep a stable voltage at the APF capacitor. A second PWM control loop forces the line supply currents to be sinusoidal and with the rms value given by (16).

III. SIMULATION RESULTS

Figs. 6 and 7 show the results obtained with this combined technology (TBC with thyristors and APF with IGBTs). The first one shows three oscillograms: Fig. 6(a) displays the three load currents, i_L^A , i_L^B , and i_L^C , which are balanced but with a lagging power factor. After the step load change in the middle of this oscillogram, these three load currents become completely unbalanced. It can be seen that the source currents shown in Fig. 6(b), remain in phase with the voltage, and always balanced, before and after the step change. The last oscillogram in Fig. 6(c) shows the contribution of the TBC, and the APF, through the currents i_Q^A , and i_F^A respectively (only phase “a” is displayed). The APF only works during the transient period, helping the line current to remain sinusoidal.

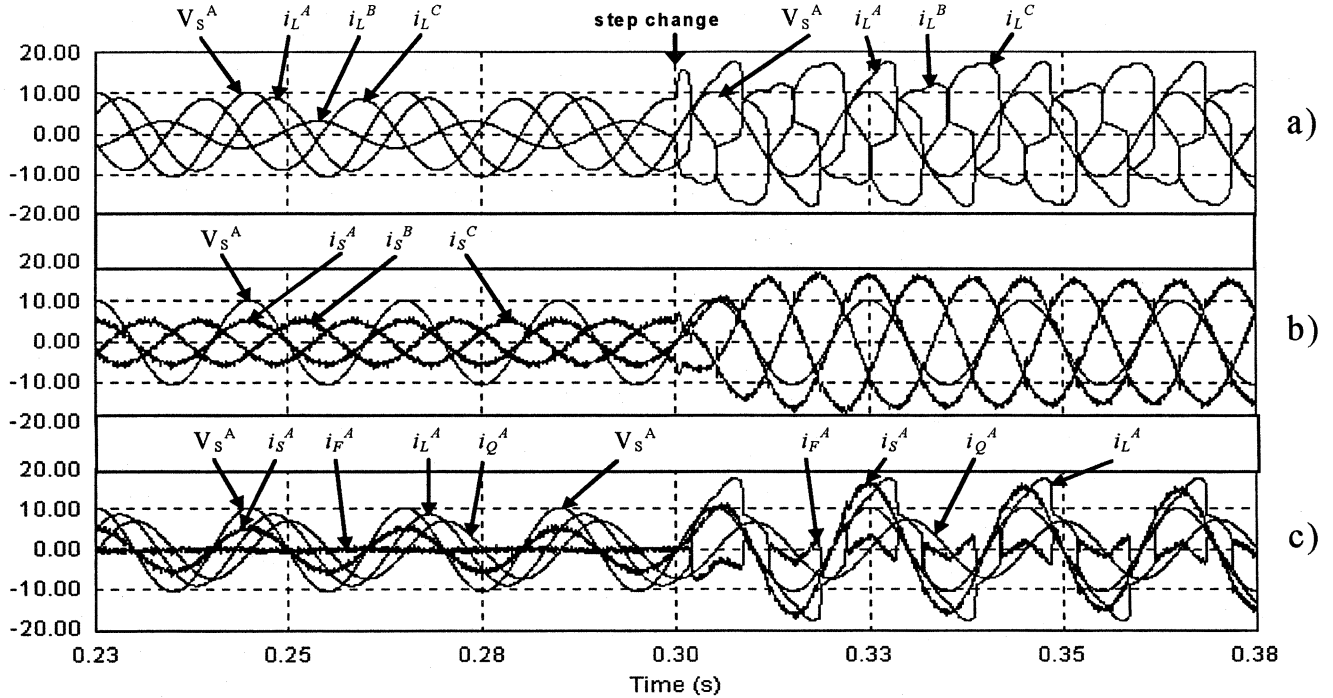


Fig. 7. Step response from unbalanced load to polluted load. (a) Load currents. (b) Source currents. (c) Phase “a” currents.

Fig. 7 shows step change from unbalanced load to polluted load. In the time indicated in the figure, a power rectifier is connected, and the load current [shown in 7(a)] becomes completely distorted and unbalanced. However, in Fig. 7(b) the three source currents i_s^A , i_s^B and i_s^C remain clean, and in phase with the corresponding source voltages V_s . Finally, the Fig. 7(c) shows the contribution of the TBC (i_Q^A), and APF (i_F^A), to clean the current of the system. Only phase “a” is shown in this last oscillogram.

In Figs. 6 and 7, the voltage V_s has been scaled 30 times smaller. The values used in the power compensator for these oscillograms were: $V_s = 220$ V (phase-to-neutral), 50 Hz. The TBC has the following compensating branches in each phase: C1 = 1.25 μ F, C2 = 2.5 μ F, C4 = 5 μ F, C8 = 10 μ F, C16 = 20 μ F, and $L = 260$ mH. These values allow compensation from -1.76 kvar to 1.76 kvar. The load parameters were: step 1) balanced load connected in delta, with $R = 160$ Ω , in parallel with $L = 500$ mH; step 2) unbalanced load connected in delta with $R_A = 400$ Ω in parallel with $L_A = 500$ mH, $R_B = 200$ Ω in parallel with a $R_{B1} - L_B$ series circuit ($R_{B1} = 1000$ Ω , $L_B = 200$ H), $R_C = 150$ Ω in parallel with $L_C = 500$ mH; step 3) polluting load with a three-phase full-wave diode rectifier, with input ac inductances $L = 0.5$ mH, and a dc load with $R = 60$ Ω , and $L = 20$ mH.

IV. EXPERIMENTAL RESULTS

An experimental prototype for the proposed topology was implemented for a nominal phase-to-phase voltage of 110 [V_{eff}], and a 1650 [VA] three-phase load. The TBC prototype includes five branches of binary scaled capacitors as shown in Table I. For economical reasons, the prototype did not include inductor branches. Then, it is only able to inject leading reactive power to the network.

TABLE I
TBC PROTOTYPE PARAMETERS

Component	Value	Unit
C1	2.5	[μ F]
C2	5.0	[μ F]
C4	10.0	[μ F]
C8	20.0	[μ F]
C16	40.0	[μ F]

TABLE II
APF PROTOTYPE PARAMETERS

Parameter	Value	Unit
L_f	5.00	[mH]
C	3,300	[μ F]
V_{REF}	160	[V _{dc}]
f_s	12	[kHz]

The APF equipment is connected in parallel to the voltage supply and their parameters are given in Table II.

It is important to notice that the switching frequency of the APF is only 12 kHz. The total harmonic distortion (THD) of the filtered currents is strongly dependent on the switching frequency of the IGBTs, and on the value of L_f . The larger L_f , the smaller the THD.

The load is a lineal balanced $R-L$ impedance in star configuration ($R_{load} = 9$ Ω , $L_{load} = 260$ mH), which is connected in parallel with a full wave diode bridge rectifier. This rectifier has an input inductance $L_D = 0.37$ mH/phase and a dc load $R = 80$ Ω .

Fig. 8 illustrates an experimental result of the TBC operation alone, which generates leading current in a binary way. Fig. 8(a)

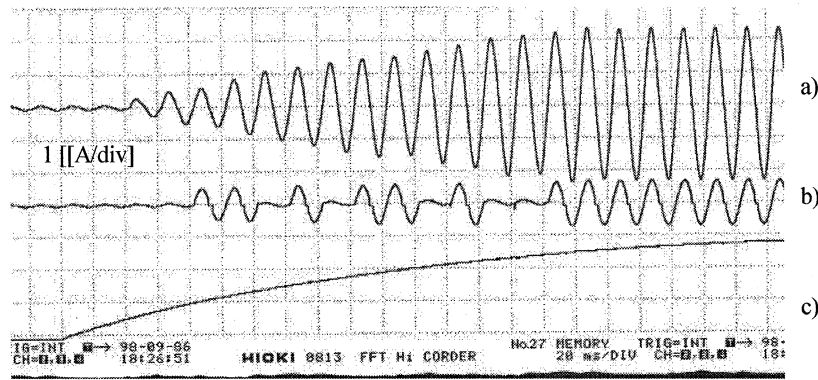


Fig. 8. Experimental TBC operation. (a) TBC current i_Q . (b) Capacitor current in the $5 \mu\text{F}$ branch. (c) Reference signal. This oscillogram shows the way the TBC generates leading current, according to the reference signal shown in (c).

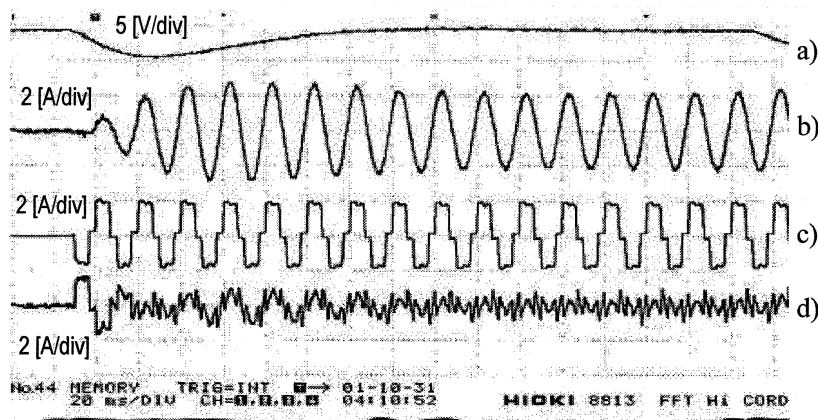


Fig. 9. Experimental APF operation. (a) APF dc-link voltage V_{DC} . (b) Line current filtered by the APF. (c) Load (rectifier) current i_L . (d) APF current i_F . This oscillogram shows the way the APF generates the harmonic currents required by the load (full-wave rectifier).

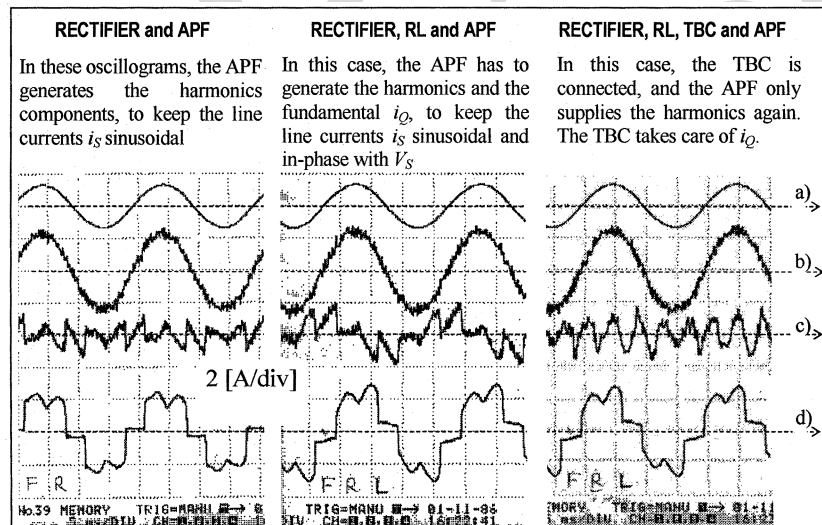


Fig. 10. Experimental TBC and APF operation. (a) Line voltage V_S . (b) Line current i_S . (c) APF current i_F . (d) Load current i_L .

shows the total leading current, Fig. 8(b) the current through the capacitor branch of $5 \mu\text{F}$, and Fig. 8(c) the reference current. On the other hand, Fig. 9 shows the typical current waveforms of the APF. Finally, Fig. 10 shows the combined action of the TBC and APF in the experimental system. The oscillogram in Fig. 10(a) shows the voltage, Fig. 10(b) the source current, Fig. 10(c) the APF current, and Fig. 10(d) the load current. The figure has been

divided into three columns. The first column of Fig. 10 shows the system with only the rectifier as a load, with the APF, and without the TBC. As can be seen, the APF is generating the harmonic currents to keep the source current sinusoidal. In the second column of Fig. 10, the RL impedance is added to the load, and the APF now has to supply the fundamental and harmonic reactive power. When the TBC is connected in the third column

of Fig. 10, the APF only supplies the harmonics, and the TBC takes care of the fundamental reactive power. In all the three situations the supply currents remain sinusoidal, but with a small ripple given by the switching frequency of the APF.

V. CONCLUSION

A combined topology, using a TBC, and a PWM-IGBT shunt APF, has been implemented. The TBC controls the power factor and corrects load unbalances. The APF eliminates the harmonics, and compensates the small amounts of power factor and unbalancing that the TBC, given its binary characteristic, is unable to correct. The two converters work independently, making the control system simple and more reliable. The system is able to compensate power factor, unbalanced loads, and harmonics, with a good dynamic response. Compared with other topologies able to do the same work, the one presented here is more economical, because the high kvar stage has been implemented with thyristors, which are cheaper than GTOs. The results obtained, show an excellent behavior under both steady-state and transient situations.

REFERENCES

- [1] L. Gyugyi, R. A. Otto, and T. H. Putman, "Principles and applications of static, thyristor-controlled shunt compensators," *IEEE Trans. Power App. Syst.*, vol. PAS-97, pp. —<AUTHOR: PAGE RANGE?>, Sept./Oct. 1978.
- [2] L. Morán, E. Mora, R. Wallace, and J. Dixon, "Line conditioning system with simple control strategy and fast dynamic response," *Proc. IEE—Generation, Transmission Distrib.*, vol. 142, no. 2, pp. 128–134, Mar. 1995.
- [3] J. W. Dixon and D. Veas, "Open loop VAR compensator, using a simple PWM pattern," *Proc. IEE—Elect. Power Applicat.*, vol. 144, no. 4, pp. 257–262, July 1997.
- [4] L. Smith, "A practical approach in substation capacitor bank applications to calculating, limiting and reducing the effects of transient current," *IEEE Trans. Ind. Applicat.*, vol. IA-12, pp. —<AUTHOR: PAGE RANGE?>, May/June 1976.
- [5] A. Ametani, "Harmonic reduction in thyristor converters by harmonic current injection," *IEEE Trans. Power App. Syst.*, vol. PAS-95, pp. —<AUTHOR: PAGE RANGE?>, <AUTHOR: MONTHS?> 1976.
- [6] J. W. Dixon, J. García, and L. Morán, "Control system for three-phase active power filter which simultaneously compensates power factor and unbalanced loads," *IEEE Trans. Ind. Electron.*, vol. 42, pp. 636–641, Dec. 1995.
- [7] J. W. Dixon, G. Venegas, and L. A. Morán, "A series active power filter based on a sinusoidal current-controlled voltage-source inverter," *IEEE Trans. Ind. Electron.*, vol. 44, pp. 612–620, Oct. 1997.
- [8] F. Z. Peng, H. Akagi, and A. Nabae, "A new approach to harmonic compensation in power systems—a combined system of shunt passive and series active filters," *IEEE Trans. Ind. Applicat.*, vol. 26, pp. 983–990, Nov./Dec. 1990.
- [9] L. Morán, L. Fernández, J. Dixon, and R. Wallace, "A simple and low cost control strategy for active power filters connected in cascade," *IEEE Trans. Ind. Electron.*, vol. 44, pp. 621–629, Oct. 1997.
- [10] C. Maffrand, J. W. Dixon, and L. Morán, "Binary controlled, static VAR compensator, based on electronically switched capacitors," in *Proc. IEEE PESC'98*, 1998, pp. 1392–1396.
- [11] I. Takahashi and G. J. Su, "A 500 Hz power system, power converter, and transmission lines," in *Conf. Rec. IEEE-IAS Annu. Meeting*, 1989, pp. 988–1002.
- [12] J. W. Dixon, J. M. Contardo, and L. A. Morán, "A fuzzy controller active front-end rectifier with current harmonic filtering characteristics and minimum sensing variables," *IEEE Trans. Power Electron.*, vol. 14, pp. —<AUTHOR: PAGE RANGE?>, July 1999.



Juan Dixon <AUTHOR: PLEASE LIST YEAR(S) AND GRADE(S) OF IEEE MEMBERSHIP> was born in Santiago, Chile. He received the degree in electrical engineering from the Universidad de Chile, Santiago, Chile, in 1977, and the M.Eng. and Ph.D. degrees from McGill University, Montreal, QC, Canada, in 1986 and 1988, respectively.

Since 1979, he has been with the Electrical Engineering Department, Pontificia Universidad Católica de Chile, Santiago, Chile, where he is currently an Associate Professor. His main areas of interests are electric vehicles technologies, electric traction, power converters, PWM rectifiers, multilevel and multistage converters, active power filters, and var compensators.

Dr. Dixon has authored more than 25 papers on power electronics, published in various IEEE TRANSACTIONS.



Yamille del Valle <AUTHOR: PLEASE LIST YEAR(S) AND GRADE(S) OF IEEE MEMBERSHIP, IF APPLICABLE> received the civil industrial engineering degree with a major in electrical engineering from the Pontificia Universidad Católica de Chile, Santiago, Chile, in 2001.

At the university, she was a Research Assistant in the Power Electronics Area. She is currently an Instructor and Researcher with the Faculty of Physical and Mathematical Sciences, Universidad de Chile, Santiago, Chile, working in the Energy Area of the Electrical Engineering Department. Her main interests include active power filters and flexible ac transmission systems.



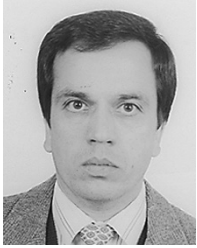
Marcos Orchard <AUTHOR: PLEASE LIST YEAR(S) AND GRADE(S) OF IEEE MEMBERSHIP, IF APPLICABLE> received the civil industrial engineering degree with a major in electrical engineering from the Pontificia Universidad Católica de Chile, Santiago, Chile, in 2001.

At the university, he was a Research Assistant in the Power Electronics and Automatic Control Areas during 2000–2001. He was then a Project Engineer with CONTAC INGENIEROS LTDA. He is currently an Instructor and an Automatic Control Researcher in the Electrical Engineering Department, Faculty of Physical and Mathematical Sciences, Universidad de Chile, Santiago, Chile. His main interests are related to fuzzy expert systems, fault detection and diagnosis, and multivariate statistical control.



Micah Ortúzar <AUTHOR: PLEASE LIST YEAR(S) AND GRADE(S) OF IEEE MEMBERSHIP, IF APPLICABLE> was born in Santiago, Chile. He received the electrical engineering degree from the Pontificia Universidad Católica de Chile, Santiago, Chile, where he is currently working toward the Ph.D. degree.

He has worked on power active filters, power electronics, and electric vehicles research projects.



Luis Morán <AUTHOR: PLEASE LIST YEAR(S) AND GRADE(S) OF IEEE MEMBERSHIP> was born in Concepción, Chile. He received the degree in electrical engineering from the Universidad de Concepción, Concepción, Chile, in 1982, and the Ph.D. degree from Concordia University, Montreal, QC, Canada, in 1990.

Since 1990, he has been with the Electrical Engineering Department, University of Concepción, where he is currently a Professor. He has extensive consulting experience in the mining industry,

especially in the application of medium-voltage ac drives, large-power cycloconverter drives for SAG mills, and power quality issues. His main areas of interests are ac drives, power quality, active power filters, FACTS, and power protection systems.

Prof. Morán has authored more than 25 papers on active power filters and static var compensators published in various IEEE TRANSACTIONS. He was the principal author of the paper that received the Outstanding Paper Award for the best paper published in the IEEE TRANSACTIONS ON INDUSTRIAL ELECTRONICS during 1995. From 1997 until 2001, he was an Associate Editor of the IEEE TRANSACTIONS ON POWER ELECTRONICS. In 1998, he received the City of Concepción Medal of Honor for achievement in applied research.



Carlos Maffrand <AUTHOR: PLEASE LIST YEAR(S) AND GRADE(S) OF IEEE MEMBERSHIP, IF APPLICABLE> was born in La Carlota, Argentina. He received the B.Eng. degree in mechanical and electrical engineering from the Universidad Nacional de Rio Cuarto (UNRC), Rio Cuarto, Argentina.

In 1983, he joined the Grupo de Electronica Aplicada (GEA). From 1986 to 1992, he was with SILEC, where he was a Software and Hardware Developer in the area of microcontrollers. His current research interests are power electronics, digital systems, microprocessor and DSP applications, and control techniques. He is currently a Professor in the area of digital systems and control systems at UNRC.

IEEE
Proof